

# MetaML-Pro: Cross-Stage Design Flow Automation for Efficient Deep Learning Acceleration

ZHIQIANG QUE, Imperial College London, UK  
 JOSE G. F. COUTINHO, Imperial College London, UK  
 CE GUO, Imperial College London, UK  
 HONGXIANG FAN, Imperial College London, UK  
 WAYNE LUK, Imperial College London, UK

This paper presents a unified framework for codifying and automating optimization strategies to efficiently deploy deep neural networks (DNNs) on resource-constrained hardware, such as FPGAs, while maintaining high performance, accuracy, and resource efficiency. Deploying DNNs on such platforms involves addressing the significant challenge of balancing performance, resource usage (e.g., DSPs and LUTs), and inference accuracy, which often requires extensive manual effort and domain expertise. Our novel approach addresses two key issues: cross-stage co-optimization and optimization search. By seamlessly integrating programmatic DNN optimization techniques with high-level synthesis (HLS)-based metaprogramming and leveraging advanced design space exploration (DSE) strategies like Bayesian optimization, the framework automates both top-down and bottom-up design flows, reducing the need for manual intervention and domain expertise. The proposed framework introduces customizable optimization, transformation, and control blocks to enhance DNN accelerator performance and resource efficiency. Experimental results demonstrate up to a 92% DSP and 89% LUT usage reduction for select networks, while preserving accuracy, along with a 15.6-fold reduction in optimization time compared to grid search. These results underscore the novelty and potential of the proposed framework for automated, resource-efficient DNN accelerator designs.

CCS Concepts: • **Hardware** → **Electronic design automation; Emerging tools and methodologies; Hardware-software codesign; Computer systems organization** → **Neural networks; Reconfigurable computing**.

Additional Key Words and Phrases: FPGAs, algorithm-hardware codesign, design automation, design space exploration

## ACM Reference Format:

Zhiqiang Que, Jose G. F. Coutinho, Ce Guo, Hongxiang Fan, and Wayne Luk. 2025. MetaML-Pro: Cross-Stage Design Flow Automation for Efficient Deep Learning Acceleration. *J. ACM* 1, 1, Article 1 (March 2025), 27 pages. <https://doi.org/10.1145/nnnnnnn.nnnnnnn>

## 1 INTRODUCTION

The field of deep learning has witnessed unprecedented growth in recent years, driven by the increasing demand for efficient and high-performance applications [19]. Consequently, FPGA-based deep neural network (DNN) accelerator design and optimization have gained significant attention [48, 50]. The development of an efficient FPGA-based DNN design requires a diverse

Authors' addresses: Zhiqiang Que, [z.que@imperial.ac.uk](mailto:z.que@imperial.ac.uk), Imperial College London, UK; Jose G. F. Coutinho, Imperial College London, UK; Ce Guo, Imperial College London, UK; Hongxiang Fan, Imperial College London, UK; Wayne Luk, [w.luk@imperial.ac.uk](mailto:w.luk@imperial.ac.uk), Imperial College London, UK.

Permission to make digital or hard copies of all or part of this work for personal or classroom use is granted without fee provided that copies are not made or distributed for profit or commercial advantage and that copies bear this notice and the full citation on the first page. Copyrights for components of this work owned by others than ACM must be honored. Abstracting with credit is permitted. To copy otherwise, or republish, to post on servers or to redistribute to lists, requires prior specific permission and/or a fee. Request permissions from [permissions@acm.org](mailto:permissions@acm.org).

© 2025 Association for Computing Machinery.

0004-5411/2025/3-ART1 \$15.00

<https://doi.org/10.1145/nnnnnnn.nnnnnnn>

skill set that combines expertise in machine learning with low-level knowledge of the target hardware architecture [35]. Optimizing these DNN designs is a complex process, as it involves balancing competing objectives. On one hand, high accuracy during inference is crucial from an application perspective. On the other hand, the design must be optimized for the underlying hardware architecture, meeting power, latency and throughput requirements while fitting into the FPGA device [5, 7]. Achieving an optimal balance between these conflicting objectives requires careful consideration and effective optimization strategies [42].

Existing optimization techniques for DNNs and hardware have a limitation in that they are often handled in separate stages, with information exchanged only in a top-down manner from the application to hardware. Manual intervention is usually required for bottom-up information flow. This information exchange between multiple stages can significantly enhance the optimization process, as application and hardware optimizations can interact and affect each other. For instance, modifying the DNN model's architecture could impact the FPGA resource utilization, and optimizing the FPGA design could influence the DNN model's accuracy [42]. In addition, there has been limited focus on combining optimization strategies targeting different abstraction levels, such as algorithmic level neural networks and High Level Synthesis (HLS) C++, hindering the selection of the most effective combination of optimization techniques for a given problem. Furthermore, little work focuses on supporting comprehensive exploration of such combination with various configurations of involved optimization techniques towards DNN accelerations.

In this paper, we address these two aforementioned technical challenges: C1 Custom Co-Optimization Strategies and C2 Cross-Stage Optimization Search. First, to navigate the vast design space of hardware-software exploration, this work employs a unique co-optimization approach encompassing three key aspects: (1) optimizing the DNN software model, (2) refining the DNN hardware architecture, and (3) exploring the design space. By encoding each optimization independently and combining them as needed, this approach enables the modular reuse and adaptation of optimizations across benchmarks and hardware platforms. Leveraging programmatic manipulation, we facilitate close coordination between DNN model and hardware design optimizations, significantly expanding the range of design choices. Advanced techniques such as Bayesian Optimization streamline the exploration of the large hardware-software design space, ensuring effective and systematic optimization [21, 31, 37].

Second, developing efficient DNN accelerators requires a coherent strategy that automates the selection, combination, and tuning of optimization techniques across multiple abstraction levels [2, 24, 46, 49]. It is challenging to identify the most effective combination, order and tuning of optimization techniques to ensure optimal outcomes [45, 50]. This work tackles these challenges by employing a cross-stage optimization search approach that coordinates the interaction between different stages of the design flow. By leveraging a combination of top-down and bottom-up optimization strategies, the framework dynamically adapts to the specific requirements of the hardware and the application, guiding the optimization process iteratively and identifying the best optimization techniques and their sequences.

This work utilizes a Bayesian guided nested-loop optimization structure involving both local and global phases, combining very distinct optimization techniques and incorporating feedback from the latter stages of the design flow to refine the process iteratively, as shown in Fig. 1. The proposed cross-stage framework operates across various computational spaces, such as software and High-Level Synthesis (HLS), and can potentially target diverse hardware platforms including FPGAs and ASICs. It supports autonomous custom optimization tasks (e.g., OPT-1 to OPT-4 and potentially more), each constrained by user-defined parameters to optimize performance.

We make the following contributions in this paper:

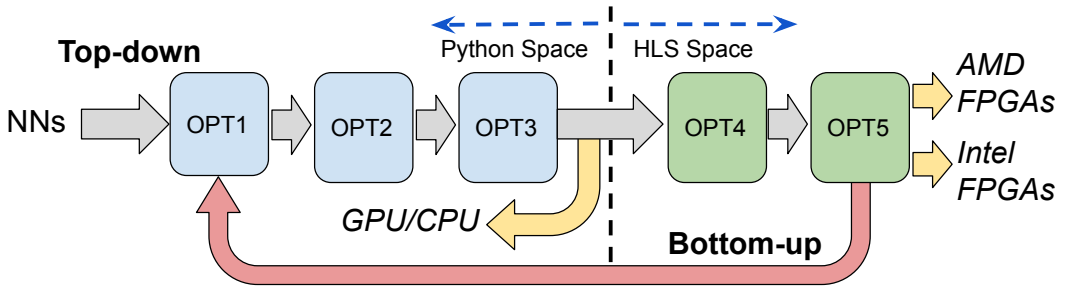


Fig. 1. The proposed approach.

- A novel co-optimization framework for FPGA-based DNN accelerators. This framework seamlessly integrates programmatic DNN optimizations with HLS-based metaprogramming, coordinated by state-of-the-art Design Space Exploration (DSE) strategies. It supports automated design iteration processes through top-down and bottom-up flows, enabling more efficient optimization and accurate performance predictions by refining DSE estimates with post-HLS data (Section 3).
- A library of reusable optimization, transformation and control tasks designed to be customizable and flexible, and that can be easily integrated into our co-optimization framework. Some of the tasks in our library are specific to certain applications and/or target technologies, while others are agnostic, providing versatility and adaptability to the framework.
- Enabling rapid development of customized cross-stage design-flows. The framework introduces novel building tasks that automate the integration and iteration of various stages in the design flow. These components allow for the automation of both high-level and low-level design processes, streamlining the development of tailored solutions for different use cases and improving decision-making accuracy in the optimization process.
- A comprehensive evaluation of the proposed framework using multiple benchmarks and different optimization strategies. This evaluation will provide insights into the effectiveness of the framework and its optimization modules under different scenarios (Section 5).

*Relationship to Prior Publications.* This paper expands on our previous studies [26, 27, 30] which primarily focus on local optimizations. In [27], we propose MetaML, an optimization framework, that customizes design flow for DNNs with local optimizations. In [26], we introduce control capabilities within the optimization framework, while [27] focuses on Quantization Heuristic Search (QHS) optimization task for compressing DNN accelerators. However, these prior works are limited in their ability to perform global optimization due to their focus on isolated optimization tasks. The inability to account for interdependencies between optimization tasks across stages mean that the overall design might not have achieved the optimal balance between accuracy, performance, and resource efficiency. This work addresses these limitations by incorporating bottom-up feedback and leveraging Bayesian optimization to enable global optimization across the entire design flow. By adjusting optimization tasks at each stage based on performance feedback, our framework ensures that each optimization choice contributes to a more cohesive and globally optimal solution. This extended approach maintains high accuracy while improving resource efficiency, specifically in resource-constrained environments. We plan to open-source MetaML-Pro to the research community, aiming to inspire further research and development in this area.

## 2 RELATED WORK

The field of FPGA-based DNN acceleration has rapidly expanded, leading to the development of numerous optimization techniques and tools. Several co-optimization techniques have been



Fig. 2. A typical FPGA design flow. This FPGA design flow begins with defining the specifications (SPEC), followed by implementing and testing the design in software (SW). If High-Level Synthesis (HLS) is used, high-level code (e.g., C/C++) is converted into hardware description language (HDL). The design then moves to the Register Transfer Level (RTL) stage, where it is described in HDL (e.g., Verilog/VHDL) and synthesized into a netlist of logic gates. Finally, the netlist is used to generate a bitstream, which is loaded onto the FPGA to configure the hardware. Each stage progressively refines the design from concept to implementation.

proposed that optimize both algorithm and hardware stages for DNNs on FPGAs, as discussed in various papers [6, 10–14, 16, 46, 49] and in hardware-aware neural architecture search studies like [2, 24]. These optimization strategies are often coupled with design space exploration, but are typically hardcoded and cannot be easily changed or customized.

Other approaches offer end-to-end software frameworks, such as Xilinx’s Vitis AI [17] and Intel’s OpenVINO [1], which optimize DNNs with pre-built optimizations for deployment on specific target technologies. However, they are not designed for easy addition of new optimization strategies or to search for the most effective combined strategies.

Furthermore, some frameworks allow developers to describe and customize DNN optimization strategies, but their scope is limited. For instance, ScaleHLS [47] and SOTA-OPT [3] focus on HLS-based optimization strategies and hardware designs, but their optimization scope is restricted to MLIR. TVM [4] is a general-purpose DNN compilation framework that offers performance portability across different types of devices, but optimizations occur solely at the graph (IR) level.

Moreover, frameworks, such as FINN [39], HLS4ML [7], and fpgaConvNet [41], provide optimized hardware building blocks for FPGA-based DNN accelerators, and allow optimization strategies to be codified using these blocks. However, they do not support automated bottom-up optimization flows, where hardware stage information guides the optimization of the application (DNN) stage.

To overcome the limitations of existing optimization techniques for DNNs and hardware, our framework derives fully automated high-level optimization flows backed by reusable target-specific and target-agnostic building blocks. Our approach enables automated top-down and bottom-up flows, allowing for the creation of customized cross-stage optimization strategies for various DNN designs. Moreover, our approach integrates new and existing optimization techniques targeting various levels of abstraction, such as neural networks through graph optimizations and HLS C++ through source-to-source optimizations [40].

### 3 OUR APPROACH

#### 3.1 Overview

In this paper, we introduce a novel framework for creating customizable design-flows that optimize FPGA-based DNNs, with a focus on automating both top-down and bottom-up flows between application and hardware optimization stages.

A design-flow represents a sequence of tasks that convert a high-level specification into a final hardware design. A design-flow is typically implemented as a multi-stage pipeline, with each stage operating on a specific model abstraction. As the pipeline progresses, the model abstraction is gradually reduced and optimized, taking into account the features of the target device. For example, a typical design-flow targeting FPGAs is shown in Fig. 2. It begins with defining specifications (SPEC) and testing the design in software (SW). If High-Level Synthesis (HLS) is used, a high-level DNN model, such as one described in TensorFlow, can be translated into a C++ HLS model using

tools like HLS4ML. This model is then converted into an RTL description (e.g., Verilog/VHDL) using tools like Vivado HLS. The RTL model is further synthesized into a netlist, which is optimized for the FPGA's architecture, and finally translated into a bitstream that configures the FPGA hardware.

Feedback information can be utilized to enable lower-stage information to refine higher-stage optimizations, employing more accurate metrics that were previously unavailable. We have developed a framework that allows users to codify fully automated optimizing design-flows with the following requirements:

- **Customizable:** Refers to the ability for users to customize, extend, or modify the design-flow to meet specific needs and support experimentation. Users can select a set of building tasks that implement optimization, transformation, or control tasks, combine them in a specific order, and fine-tune their parameters to generate a specific optimization flow. Additionally, they can create their own tasks and integrate them into their design-flow (see **C1**);
- **Multi-level:** Refers to the scope of optimizations and the ability to target multiple levels of abstraction, typically associated with different stages of a design-flow. For instance, optimizations operating at the Neural Network level are performed at the graph-level, while optimizations at the HLS C++ level are performed using source-level transformations (see **C1**);
- **Cross-stage:** Refers to the capability of a design-flow to support top-down and bottom-up flows between optimization stages, such as software and hardware, respectively (see **C2**).

This work focuses on custom optimizations in the SW and HLS stages while using default configuration for the remaining stages, however, the same concepts can be extended to the other stages, which is left for future work.

### 3.2 Architecture

Fig. 3 illustrates the key architectural components of a programmatically generated design flow using our approach, which comprises two main components: the pipe task and the meta-model.

The pipe task is the fundamental building block of the design flow and is responsible for implementing specific a task, such as optimization or control. By connecting pipe tasks, we create a complete design flow. The design flow's internal architecture is represented by a cyclic directed graph, where nodes represent tasks, and edges represent **paths** between tasks. A path represents a dependency between two tasks, such that a task can only be executed if its dependencies have finished executing.

The meta-model, on the other hand, is responsible for storing all of the design flow's states, including the configuration parameters of each pipe task and their respective outputs. Instead of communicating directly with each other, pipe tasks share information through the meta-model, which serves as a shared space. The meta-model has three sections, as illustrated in Fig. 3(b): configuration, log and model space.

The configuration section (**CFG**) is a key-value store that keeps the parameters of all pipe tasks in the design flow. These parameters can configure all pipe tasks of the same type or specific instances, and they can be supplied by the user or automatically modified by the pipe tasks as part of an automated tuning process. The log section (**LOG**) stores the runtime execution trace of the design flow. This section can be useful for debugging and understanding the execution flow of the design.

Finally, the **model space** stores the models generated during the execution of a design flow. Each stored model is versioned, and models derived by different stages can coexist in the same model space. In the example shown in the figure, we have stored six models covering three abstraction levels: DNN, HLS C++ , and RTL. Each model in the model space encapsulates all its supporting files, tool reports, and computed metrics. Moreover, they can be accessed and manipulated by any pipe task in the design flow, enabling cross-stage optimizations.

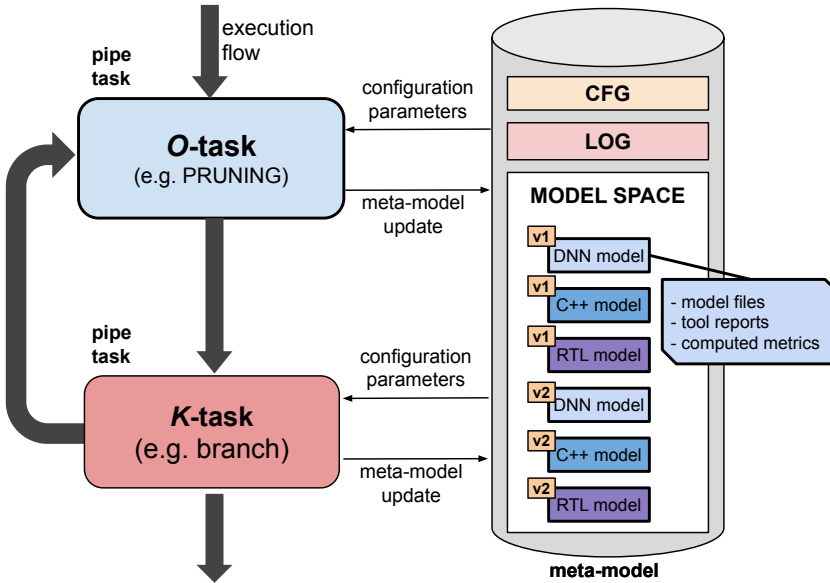


Fig. 3. A connection between a *O*-task and a *K*-task. A pipe task has a uniform interface allowing any two pipe tasks to be connected (although there may be constraints about how many connections a task can handle). A *O*-task typically enhances DNN models based on specific objectives and constraints. A *K*-task on the other hand, manages the control flow. Each connection defines a unidirectional stream between a source task and a target task.

### 3.3 Reusable Pipe Tasks

Table 1 presents a list of pipe tasks that have been implemented in our approach, along with their roles, multiplicity, and parameters. The multiplicity denotes the number of input and output channels that a task can handle. We classify pipe tasks into three types based on their roles:

- ***K*-task:** These are generic tasks that control top-down and bottom-up flows. Examples include: **BRANCH**, which selects an output path at runtime based on a boolean condition; **JOIN**, which merges multiple paths into one; **FORK**, which allows multiple concurrent strategy paths; **REDUCE**, which consolidates the results of multiple strategy paths into one; and **STOP**, which terminates the design flow;
- ***O*-task:** These are self-contained optimizing tasks that enhance deep learning models based on specific objectives and constraints. Our current pipe task repository includes **PRUNING** and **SCALING**, which are implemented using the Keras API (version 2.9.0), and **QUANTIZATION**, which is performed using C++ source-to-source transformations via the Artisan framework [40];
- **$\lambda$ -task:** These tasks perform functional transformations on the model space, such as compilation and synthesis. Examples include **HLS4ML** (version 0.6.0), which translates a DNN model into an HLS C++ model, and **Vivado HLS** (version 20.1), which translates an HLS C++ model into an RTL model.

It is worth noting that our framework is customizable, allowing users to create and integrate their own pipe tasks tailored to their specific needs.

### 3.4 Building a Strategy

Listing.1 provides the Python code for implementing the pruning strategy depicted in Fig.7(a) and discussed in Section 5.2. The code consists of three sections: (i) lines 4–9 builds the design-flow

Table 1. A list of implemented pipe tasks.

Type	Role	Multiplicity	Parameters
JOIN	$K$	many-to-1	-
BRANCH	$K$	1-to-2	fn: meta-model $\rightarrow$ bool
FORK	$K$	1-to-many	-
REDUCE	$K$	many-to-1	fn: [meta-model] $\rightarrow$ meta-model
STOP	$K$	1-to-0	fn: meta-model $\rightarrow$ output
HLS4ML	$\lambda$	1-to-1	default_precision IOType FPGA_part_number clock_period test_dataset
VIVADO-HLS	$\lambda$	1-to-1	project_dir
INTEL-oneAPI	$\lambda$	1-to-1	project_dir
KERAS-MODEL-GEN	$\lambda$	0-to-1	train_en train_test_dataset train_epochs
PRUNING	$O$	1-to-1	tolerate_acc_loss ( $\alpha_p$ ) pruning_rate_thresh ( $\beta_p$ ) train_test_dataset train_epochs
SCALING	$O$	1-to-1	default_scale_factor tolerate_acc_loss ( $\alpha_s$ ) scale_auto max_trials_num train_test_dataset train_epochs
QUANTIZATION	$O$	1-to-1	tolerate_acc_loss ( $\alpha_q$ ) train_test_dataset

architecture graph by connecting the corresponding tasks. The  $\gg$  and  $\ll$  operators are utilized to define the connections between task instances, and the default name of each task instance serves as its identifier, although it can be overridden by providing it as an argument (line 6). The end result is a cyclic-directed graph. **(ii)** lines 11–23 define the configuration object, which holds all the parameters for configuring the tasks. Parameters referred to as `TaskType::parameter` are passed to all tasks of that task type (lines 16–19), whereas parameter names in the format of `InstanceName@parameter` are passed to a specific instance (line 15). All other parameters are global (lines 20–21) and accessible to any task. Finally, **(iii)** line 25 executes the design-flow by passing the configuration object.

The execution of the design-flow starts with graph validation, which ensures that there is at least one source task and no multiplicity constraints are violated. Tasks are executed by an internal scheduler using a thread pool, which assigns jobs to available workers or stalls until a worker

```

1 # The pruning strategy architecture - Fig. 2(a)
2 from MetaML import *
3 # design-flow architecture
4 with Dataflow() as df:
5     join = Join() << KerasModelGen()
6     branch = Branch('B') << (VivadoHLS() <<
7         (HLSML() << (Pruning() << join)))
8
9     branch >> [join, Stop()]
10 # design-flow configuration
11 cfg = {
12     'KerasModelGen::train_en': False,
13     'Pruning::tolerate_accuracy_loss': 0.02,
14     'Pruning::pruning_rate_threshold': 0.02,
15     'B@fn': lambda metamodel: ...
16     'HLS4ML::default_precision': 'ap_fixed<18,8>',
17     'HLS4ML::IOType': 'io_parallel',
18     'HLS4ML::FPGA_part_number': 'xc7z020c1g400-1',
19     'HLS4ML::clock_period': 10,
20     'train_test_dataset': '/mypath/target_dataset',
21     'train_epochs': 15,
22     'Stop::fn': lambda metamodel: ...
23 }
24 # run design-flow
25 optimised_model = df.run(cfg)

```

Listing 1. The implementation of the pruning strategy using our framework.

becomes available. After validating the architecture graph, an empty meta-model is generated using the supplied configuration, and the scheduler runs the source task. When a task completes execution, it submits a job to execute the next set of tasks in the flow. The STOP task terminates execution when all submitted jobs are completed. Modifying the design-flow architecture and updating its configuration parameters can lead to new optimization strategies, which is discussed next.

## 4 IMPLEMENTATION

### 4.1 Auto-Pruning Algorithm with Binary Search

Pruning is a technique that improves the performance and efficiency of neural networks by removing insignificant weights. The pruning strategy uses a PRUNING  $O$ -task, which gradually zeroes out weights during training to create a more compact and efficient network while maintaining accuracy. This optimization task supports auto-pruning, which automatically determines the highest pruning rate while maintaining a given level of accuracy loss. The PRUNING  $O$ -task is illustrated in Fig. 7(a). Formally, the objective of this  $O$ -task is defined as:

$$\begin{aligned}
 & \text{maximum } Pruning\_rate \\
 & \text{subject to } Accuracy\_loss(Pruning\_rate) \leq \alpha_p
 \end{aligned} \tag{1}$$

Starting at 0% pruning rate, the auto-pruning algorithm obtains initial accuracy  $Acc_{p_0}$  at step 1 ( $s_1$ ). It then uses a binary search approach, increasing or decreasing the pruning rate based on whether the accuracy loss is within a user-defined tolerance ( $\leq \alpha_p$ ). The algorithm terminates when the rate difference is below a threshold ( $\beta_p$ ). The number of steps is determined by  $1 + \log_2(1/\beta_p)$ .



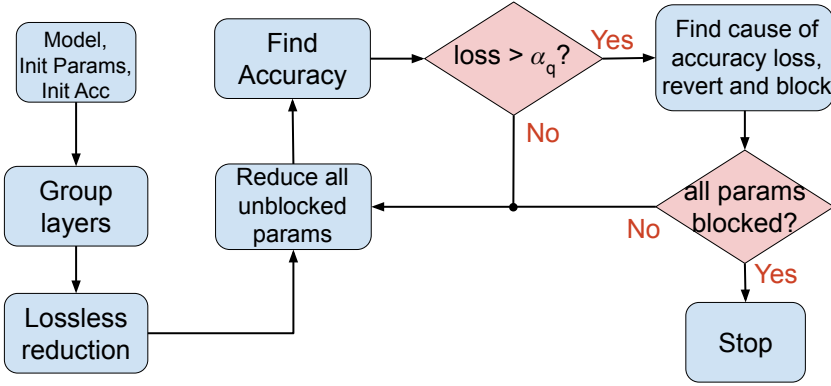


Fig. 4. The proposed QHS algorithm

Algorithm search steps and direction are shown in Fig. 8. Both the tolerance ( $\leq \alpha_p$ ) and threshold ( $\beta_p$ ) values are initially set to 2% in this work.

#### 4.2 Quantization Heuristic Search (QHS) algorithm

The optimization task with the proposed QHS algorithm operates at the HLS C++ level, modifying the fixed-point numerical representations directly at C++ source-level. At this level, there is more direct control over hardware optimizations, resulting in fewer unintended side-effects than making changes at a higher level. This task supports auto quantization, which automatically determines the lowest bitwidth for each layer while maintaining a given level of accuracy loss. Formally, the objective of this task is defined as:

$$\begin{aligned} & \text{maximum} && \textit{Bit\_width\_reduction} \\ & \text{subject to} && \textit{Accuracy\_loss}(\textit{Bit\_width\_reduction}) \leq \alpha_q \end{aligned} \quad (2)$$

It performs mixed-precision quantization for DNNs, allowing separate precisions for the weights, biases and results of layers of a model, taking the advantages of the customizability of FPGAs. While this customizability creates a massive search space of quantization configurations, dependencies within the network can be used to reduce the degrees of freedom of the design space. While other efforts target inter-layer mixed-precision quantization algorithms, our meta-programming based approach programmatically groups a number of cascaded layers described in HLS C++ into one virtual layer based on specific assumptions to reduce the complexity and improve efficiency of this optimization task. For example, if the output of a convolutional layer is 8 bits, there is no benefit in having a directly subsequent max-pooling layer with a 16-bit width. Conversely, if the max-pooling layer requires a bit-width of 4, an equivalently accurate and more efficient design would set the bit-width of the preceding convolutional layer to 4 as well. This work automatically compacts a model into a series of virtual layers using these dependencies. These virtual layers are constructed by grouping weight-layers, such as convolutional or FC layers, together with batch-normalization, pooling, and activation functions on their outputs.

Fig. 4 shows the steps of the proposed QHS algorithm. The optimization task begins by accepting a model with a maximum tolerable accuracy loss, denoted as  $\alpha_q$ . Initially, virtual layers are created, and lossless reduction is performed by minimizing the integer bits representing model parameters using the base-2 logarithm of the largest weight and bias in each layer, plus one bit for the sign to avoid saturation. Subsequently, all parameters (weights, biases and results) are initially assumed to be further reducible. The total bit-widths of these parameters are then reduced by one bit if they are considered reducible. This quantization is applied to the C++ kernel, and the accuracy is evaluated

through a runtime simulation. If the accuracy loss remains within the user-specified tolerance,  $\alpha_q$ , this step is repeated. If the accuracy loss exceeds the tolerance, the algorithm identifies and blocks non-reducible precisions. It determines which precisions are most sensitive by testing the reduction impact on accuracy. If a bit-width reduction breaks the accuracy constraint, that precision is marked non-reducible. The process repeats until no further reductions are possible within the accuracy constraints.

### 4.3 Scaling Algorithm.

To accommodate a large DNN design on an FPGA, we use the SCALING *O*-task that automatically reduces the layer size while tracking the accuracy loss  $\alpha_s$ . The search stops either when the loss exceeds  $\alpha_s$ . If necessary,  $\alpha_s$  can be adjusted to achieve further size reduction with minimal impact on accuracy.

### 4.4 Co-Optimization Workflow

As illustrated in Fig. 5, our co-optimization approach is unique in its ability to programmatically encode three types of optimizations. At the top level, a DSE optimization program is employed, executing a comprehensive exploration strategy and overseeing local optimizations at two (or more) distinct levels of abstraction. At the software DNN level, optimizations are executed on the architecture using tools like Tensorflow or PyTorch. At the HLS DNN level, optimizations are conducted by modifying the HLS code automatically using metaprogramming. Optimizing DNN models across multiple abstraction levels, from software to hardware, leverages complementary strategies that address different bottlenecks within the system. Software optimizations prioritize algorithmic efficiency and reducing computational complexity, while hardware optimizations target improvements in throughput, latency, resource utilization and energy efficiency.

Our co-optimization workflow (Fig. 5) begins with the Exploration space. Here, a DSE program utilizes a DNN model, training data, and configuration parameters to conduct the exploration workflow. This process yields a variety of hardware designs with trade-offs in metrics such as performance and accuracy. A controller process orchestrates this exploration by managing communication between the DSE program and local optimization spaces. Prior to exploration, the DSE program sets up and deploys optimization programs within these spaces. Fig. 5 depicts two such spaces: one for software (SW) utilizing TensorFlow and another for HLS employing Vivado HLS. Each space optimizes the model according to selected strategies, such as pruning or quantization.

After system setup, the exploration loop commences. In each iteration: ① The DSE program dispatches the DNN model and a specific parameter set to the software optimization space, where tasks like scaling and pruning are executed. ② Upon optimization completion, the refined model is returned to the controller along with its associated accuracy. ③ Subsequently, the model is forwarded to the HLS space for additional optimization. A metaprogram adjusts the source code based on recommended optimizations (e.g., quantization) and parameter values from the controller. After synthesis, metrics such as power, area, and accuracy are obtained and ④ fed back to the Exploration space. The DSE program evaluates designs using these metrics, retains promising candidates, and suggests new parameters for the next iteration.

This separation of concerns into distinct optimization spaces—software, HLS, and DSE—allows for the integration of diverse optimization strategies and techniques. It enables the introduction of faster or more effective exploration methods without altering existing optimizations. In addition, it combines exploration across software and hardware domains to identify effective techniques for optimizing performance. Moreover, it facilitates specialization of new hardware optimizations specific to certain FPGA HLS tools by allowing HLS code to be customized through metaprogramming.

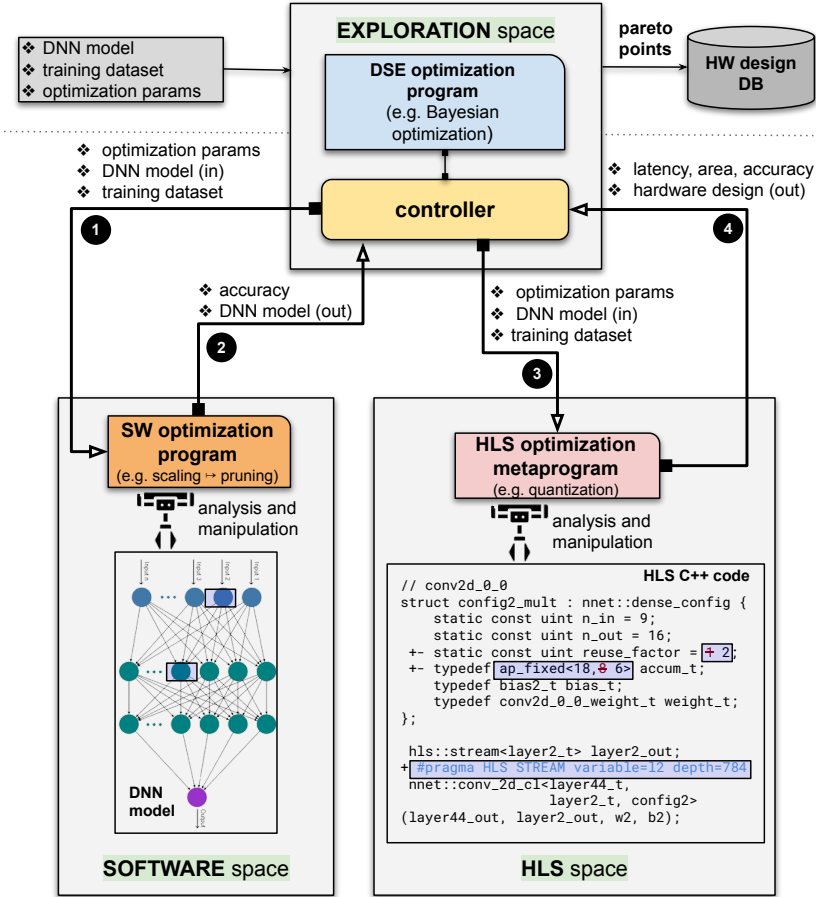


Fig. 5. This figure illustrates the implementation of our co-optimization framework, featuring an organized system of *optimization spaces*, each autonomously running Python programs within dedicated environments, overseen by an *exploration space* executing a general optimization strategy. The diagram depicts the orchestration of local optimization spaces, such as software and hardware, through a controller process.

#### 4.5 Metaprogramming based Design Optimization

A novel aspect of our co-optimization approach, as previously mentioned, is the integration of *metaprogramming* into hardware design optimization, diverging from traditional reliance solely on hardware templates (see Fig. 6(a)). These templates, crafted by hardware experts, are inherently limited in generating design variants from a predefined set of parameter values, and require expertise for extending or accommodating new DNN architectures.

In contrast, our approach optimizes hardware design architecture by programmatically modifying unoptimized High-Level Synthesis (HLS) C++ code using Python, expanding the range of possibilities beyond parameter values to generate diverse design variants. This manipulation encompasses tasks such as adjusting HLS pragmas, code restructuring for complexity reduction or performance enhancement, data type alterations for quantization support, and utilization of specialized libraries tailored for specific FPGA devices [40] (see HLS space in Fig. 5).

Figure 6(b) illustrates an HLS metaprogram in pseudocode for clarity. Metaprograms are able to analyze and instrument C++ code, creating hardware design variants to be considered during

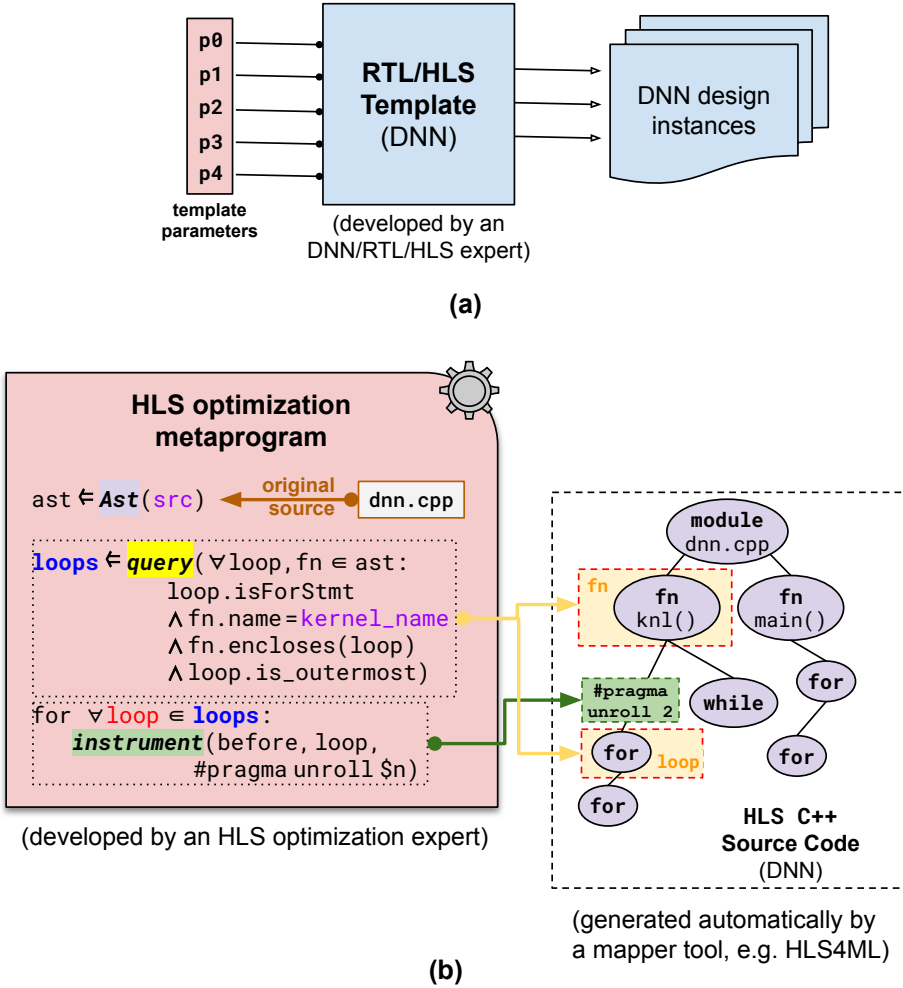


Fig. 6. (a) Current methods for deriving hardware designs rely on templates developed by experts. However, these templates are constrained in generating a finite number of design variants from predetermined parameter values and demand expertise for accommodating new DNN architectures. (b) An HLS metaprogram in pseudocode illustrating dynamic C++ code manipulation through Abstract Syntax Tree construction to derive an optimized design variant.

the Design Space Exploration (DSE) process. Hence, in our context, a metaprogram is a program that takes as input a C++ program and generates a C++ code variant using source-to-source transformations. In this example, the metaprogram creates a variant by adding an unroll pragma to all outermost for-loops in the kernel function of the original code. The key steps of the metaprogram include: (1) constructing an Abstract Syntax Tree (AST) representation of the C++ code; (2) searching for node pairs (loop, function) in the AST that meet specific criteria; and (3) iterating through the identified loops to insert the pragma code before the loop construct. A more detailed explanation about querying and instrumentation capabilities can be found in [40].

#### 4.6 Design Space Exploration (DSE)

Within our approach, Design Space Exploration (DSE) algorithms are critical for automatically adjusting the optimization parameters in subsequent iterations to improve design performance, while maintaining high model accuracy and meeting the constraints of the device.

Bayesian optimization is a key algorithm we utilize for global optimization of expensive-to-evaluate functions (represented as  $f(x)$ ). It models the objective function using a probabilistic model (e.g., Gaussian Process) and uses an acquisition function to decide where to sample next, balancing exploration of the design space with exploitation of known optimized configurations. In our context,  $x$  denotes the array of configuration settings, which serve as parameters for each optimization task within our framework. The process guides towards the most promising configurations for evaluation until a predetermined number of iterations is reached.

Our performance metrics encompass accuracy, hardware resource utilization, and adherence to operational constraints. We leverage hardware usage data obtained through Xilinx Vivado, including latency, DSP, LUT, FF, and BRAM, to inform our optimization strategy for model deployment, adjusting the optimization parameters including scaling, pruning, and quantization thresholds ( $\alpha_{p/s/q}$ ). Due to the heterogeneity of these metrics, direct summation is impractical, necessitating normalization to standardize them. This normalization technique is widely applied in various DSE methods [34].

Moreover, when optimizing a complex system, such as FPGA-based DNN accelerators, practical constraints must be considered. These constraints may arise from hardware limitations, performance requirements, and other critical factors. Incorporating these constraints into the Bayesian optimization process ensures that our search for the optimal solution occurs within a feasible and practical region of the design space. For hardware utilization constraints, a score becomes a negative maximum integer when the utilization is higher than a predefined threshold. This signals the Bayesian algorithm that the input parameter is unsuitable, steering the optimization away from poor configurations. The same approach applies to model accuracy constraint. The pseudocode of Bayesian score algorithm is shown below:

```

if (Bayesian constraints not met) then
     $f(x) = -sys.maxsize$ 
else
     $f(x) = \sum_{x \in \{Acc., DSP, LUT, BRAM\}} Norm\_Results[x] \times W[x]$ 

```

The algorithm assigns weights ( $W[\text{metric}]$ ) to each metric to indicate their relative importance.

### 5 EVALUATION

In this section, we demonstrate how optimization strategies can be built by revising design-flow architectures, combining and reusing pipe tasks, and modifying their configuration (Sections 5.2 and 5.3). We explain flow control in Sections 5.6 and 5.5. We discuss optimisation search strategies and compare evaluation results with other approaches in Sections 5.7 and Section 5.10, respectively.

#### 5.1 Experimental Setup

Experiments were conducted in Python 3.9.15 with benchmark workloads from typical DNN applications, as presented in Table 2), including jet identification [7, 22], image classification using VGG[33] and ResNet [15] networks. The jet identification task targeted FPGA-based CERN Large Hadron Collider (LHC) triggers with a 40 MHz input rate and a response latency of less than 1 microsecond. Default frequencies were 100MHz for Zynq 7020 and 200MHz for Alveo U250 and VU9P, and the HLS4ML task used 18-bit fixed-point precision with 8 integer bits.

Table 2. Benchmarks used in this work

Model Name	Dataset	Application Domain
Jet-DNN [5, 7] / Jet-CNN	Jet-HLF [7]	Jet Identification (Particle Physics)
VGG-7 [33, 36]	MNIST [20]	Image Classification
ResNet-9 [9, 15]	SVHN [23]	Image Classification
LSTM [28]	MNIST	Sequence classification

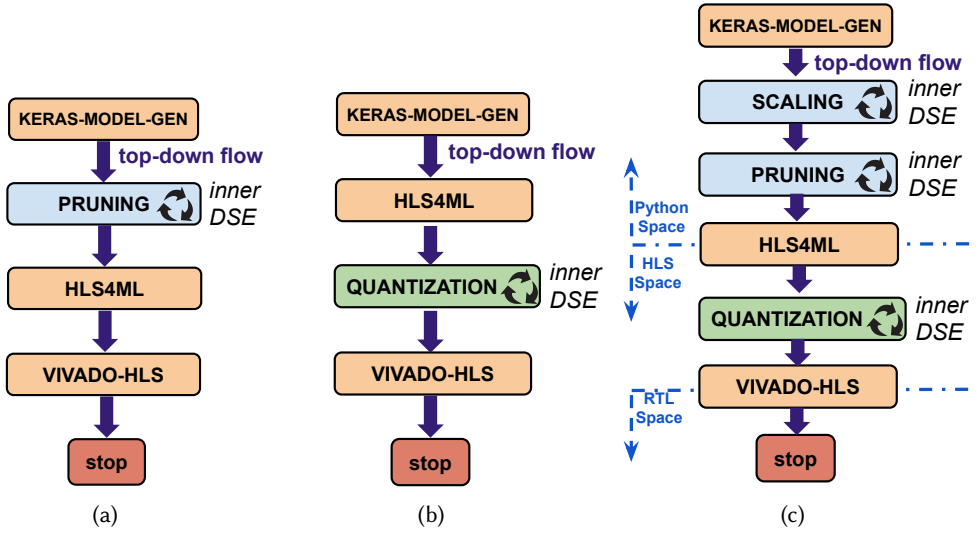
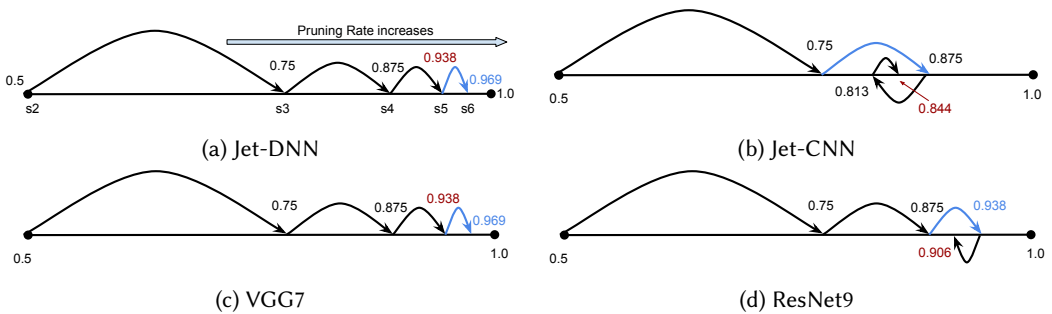


Fig. 7. (a) Pruning strategy. (b) Quantization strategy. (c) The combined strategy of scaling, pruning and quantization.

Fig. 8. The auto-pruning algorithm applied to models with binary search direction shown. Omitting step  $s_1$  for visibility. The blue arrow indicates an accuracy loss  $>$  user threshold; red denotes the optimal pruning rate.

## 5.2 Optimization Strategy using Single $O$ -task

In this subsection, we focus on three strategies which are backed by a single  $O$ -task each, respectively.

**5.2.1 Pruning strategy.** The effectiveness of the auto-pruning algorithm is demonstrated in Fig. 9. Figures (a) and (c) depict the pruning rate and accuracy for Jet-DNN and ResNet9 in each step, while

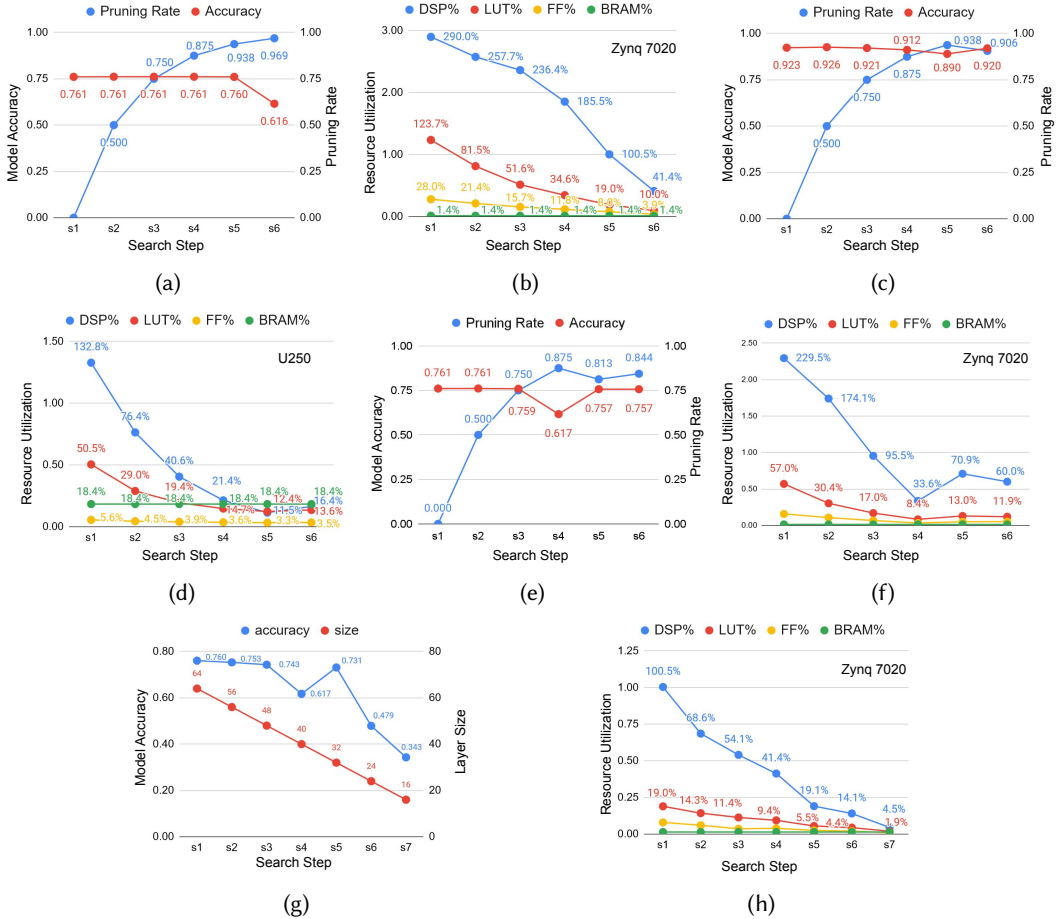


Fig. 9. (a) Pruning rates & accuracy of Jet-DNN. (b) Resource utilization of Jet-DNN design candidates after pruning. (c) Pruning rates & accuracy of ResNet9. (d) Resource utilization of ResNet9 design candidates after pruning. (e) Jet-DNN pruning rates & accuracy with scaling → pruning. (f) Resource utilization of Jet-DNN design candidates in (e). (g) Jet-DNN pruning rates & accuracy with pruning → scaling. (h) Resource utilization of Jet-DNN design candidates in (g).

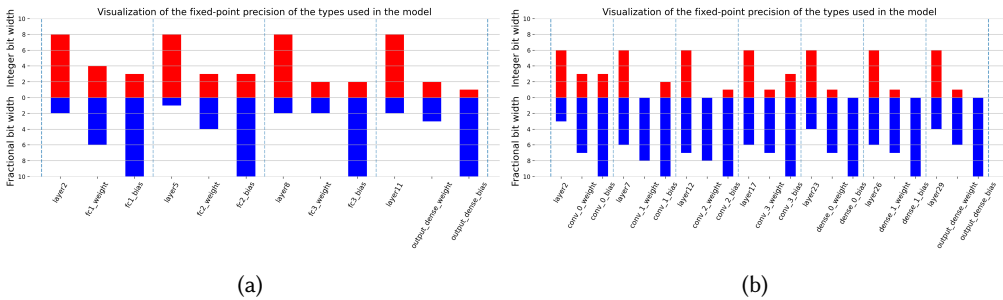


Fig. 10. (a) Quantized bitwidth of each layers in VGG7. (b) Quantized bitwidth of each layers in JetDNN.

Table 3. Results of designs with the quantization strategy using different  $\alpha_q$ . VGG7 designs are using U250 while JetDNN designs are using Zynq 7020.

Model	$\alpha_q$	DSP	LUT	FF	Acc
VGG7 Baseline	-	<b>4568</b> <b>37.2%</b>	345k 20.0%	65k 1.9%	98.2%
VGG7 Quant.	0.01	<b>934</b> <b>7.6%</b>	313k 18.1%	51k 1.5%	97.5%
VGG7 Quant.	0.05	<b>505</b> <b>4.1%</b>	318k 18.4%	66k 1.9%	93.9%
JetDNN Baseline [27]	-	<b>638</b> <b>290%</b>	66k 124%	30k 28%	76.1%
JetDNN Quant.	0.01	<b>75</b> <b>34.1%</b>	57k 107%	17k 16%	75.5%
JetDNN Quant.	0.05	<b>61</b> <b>27.7%</b>	76k 144%	7.2k 6.8%	71.6%

(b) and (d) show the resources utilization on Zynq 7020 and U250. As the pruning rate increases, hardware resource requirements, particularly DSPs and LUTs, decrease, leading to improved FPGA performance. The design candidate with the highest pruning rate within the allowed tolerance is selected.

**5.2.2 Scaling strategy.** To accommodate a large DNN design on an FPGA, we use the SCALING *O*-task that automatically reduces the layer size while tracking the accuracy loss  $\alpha_s$ . The search stops either when the loss exceeds  $\alpha_s$ . If necessary,  $\alpha_s$  can be adjusted to achieve further size reduction with minimal impact on accuracy. This work sets  $\alpha_s$  to 0.05%, which allows for model size reduction with negligible accuracy loss.

**5.2.3 Quantization strategy.** This section showcases the evaluation results of the quantization (**Q**) optimization applied to multiple DNN models within the hardware (HLS) optimization space.

Fig 10 shows the precision of the weights, biases and output of each virtual layer of the VGG7 model after being tuned by the quantization strategy with  $\alpha_q$  set to 1%. Table 3 shows how the quantization affected key evaluation metrics relating to the performance and resource usage of 2 DNN designs. With  $\alpha_q$  set to 1%, the proposed QHS quantization algorithm reduces DSP usage by a factor of 4.9 for the VGG7 model, and 8.5 for the JetDNN model. When  $\alpha_q$  is increased to 5%, the designs are further compacted, but with a larger real accuracy loss. This table highlights how varying  $\alpha_q$  levels affect model accuracy, DSP, LUT, and FF usage, illustrating the trade-offs between resource savings and accuracy as well as the effectiveness of the proposed QHS quantization algorithm.

### 5.3 Custom Optimization Strategy using Multiple *O*-tasks

With our framework, new strategies can be derived by building and revising a design-flow architecture. For instance, by inserting a scaling *O*-task before the pruning *O*-task in Fig. 7(a), a custom combined strategy can be created with results shown in Fig. 9(e) and (f). The new optimal pruning rate is 84.4% (Fig. 7(e)), lower than the previous 93.8% (Fig. 7(a)), due to reduced redundancy from the preceding scaling task. By switching the order of the *O*-tasks, a different optimization strategy performing pruning-then-scaling (pruning  $\rightarrow$  scaling) is achieved, resulting in a 0.7% accuracy



drop after one scaling step, as seen in Fig. 9(g). Moreover, the three optimization  $O$ -tasks, pruning, scaling, and quantization, can be integrated into a single automated cross-stage strategy to enhance both performance and hardware efficiency, as illustrated in Fig. 7(c). We discuss the effects of different design-flow architectures with various combinations and orders in Section 5.7, and various tolerable loss in Section 5.8

#### 5.4 Branching Flow

Fig. 11(a) illustrates a design flow that performs pruning for two alternate targets using the BRANCH  $K$ -task, for AMD/Xilinx FPGAs and Intel FPGAs. A user-defined selection function is supplied as a parameter to the BRANCH  $K$ -task which encodes a strategy determining the path forward for the design.

Fig. 12 presents the results of applying this design flow to an LSTM model on the MNIST dataset. Specifically, Fig. 12(a) illustrates the pruning rate and accuracy at each step using the PRUNING  $O$ -task. The tolerance is set to less than  $\alpha_p$  (2%) in this design. Figs 12(b) and (c) show the resource utilization of the LSTM design after each pruning step respectively on an AMD KU115 FPGA and on an Intel A10 1150 FPGA. The DSP consumption is reduced from 6011 (108%) to 2101 (38.1%) on the AMD FPGA after the final pruning rate is optimized to be 71.9%. Compared to AMD's HLS compiler, which prefers DSP blocks, Intel's HLS compiler tends to favor the use of soft multipliers for implementation. As shown in Fig 12(c), most of the computation kernels are implemented using logic resources rather than DSP blocks.

While this design flow currently supports two types of FPGAs, it can be extended to include additional paths such as GPU, CPU and ASIC technologies. Moreover, this evaluation underscores the

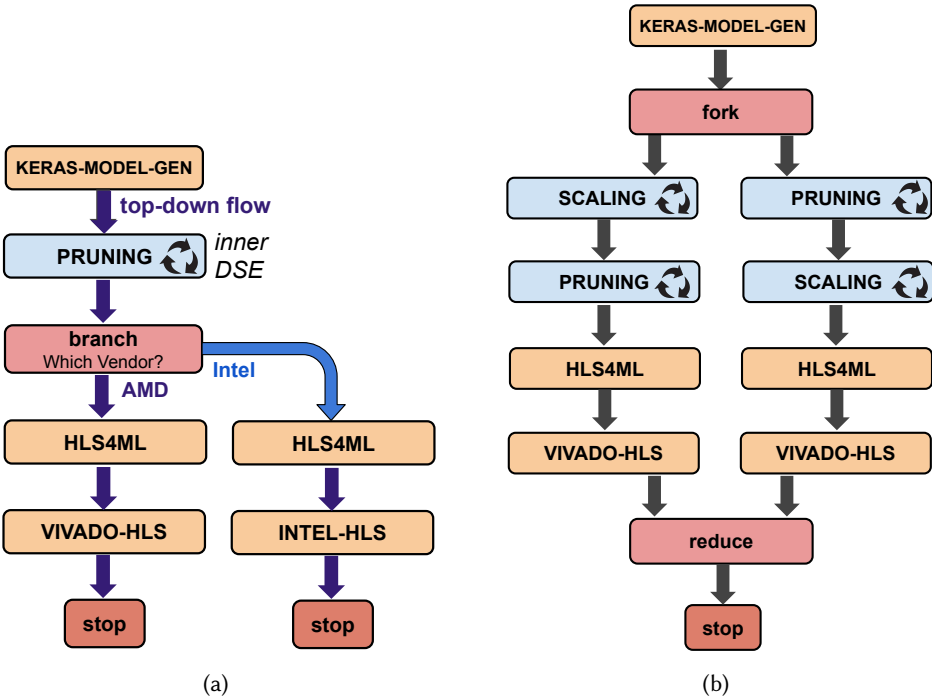


Fig. 11. (a) Pruning optimization targeting different vendors using the BRANCH  $K$ -task; (b) Combined strategy of scaling and pruning, exploring the order of  $O$ -tasks.

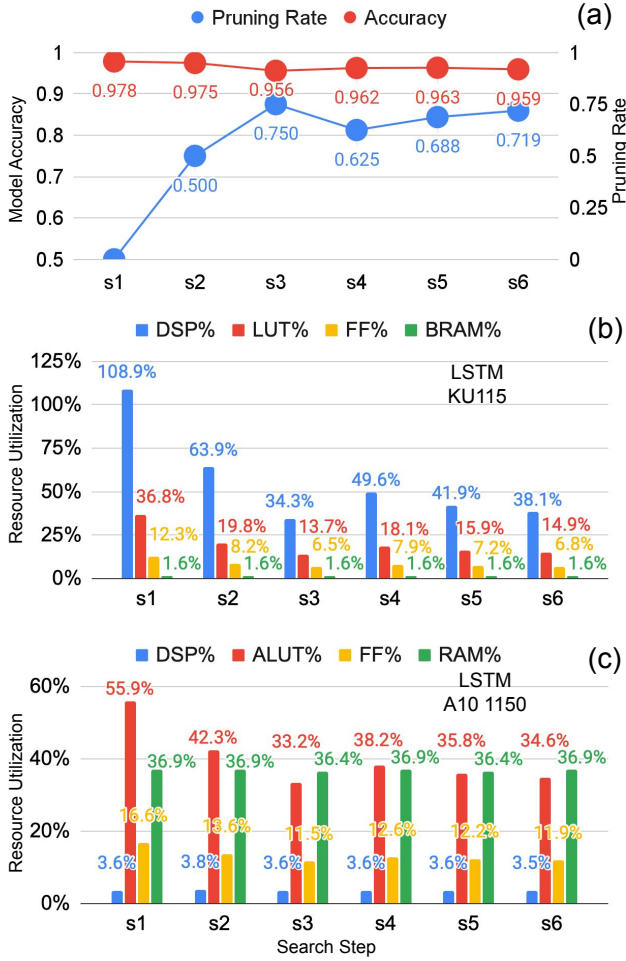


Fig. 12. LSTM model optimization on two FPGA platforms: (a) pruning rate and model accuracy using the PRUNING  $O$ -task; (b) resource utilization on an AMD KU115 FPGA; (c) resource utilization on an Intel A10 1150 FPGA.

flexibility of our approach in utilizing the same software optimization task, specifically PRUNING, across multiple hardware targets.

## 5.5 Parallel Flows

Our framework enables the execution of multiple optimization paths in parallel, allowing the selection of the best outcome among them. In Fig. 11(b), we show a design-flow with two parallel paths, where the execution order of two  $O$ -tasks is changed: scaling  $\rightarrow$  pruning and pruning  $\rightarrow$  scaling. To support parallel branches, we use the FORK task to connect multiple strategy paths. The results from each path are then evaluated based on predefined criteria, such as accuracy or resource utilization, using the REDUCE task. For this strategy, a Pareto analysis was performed on the designs resulting from both paths, as shown in Fig. 13. By employing this design-flow, designers can explore various optimization combinations and sequences when the outcomes of these strategies are not clear.

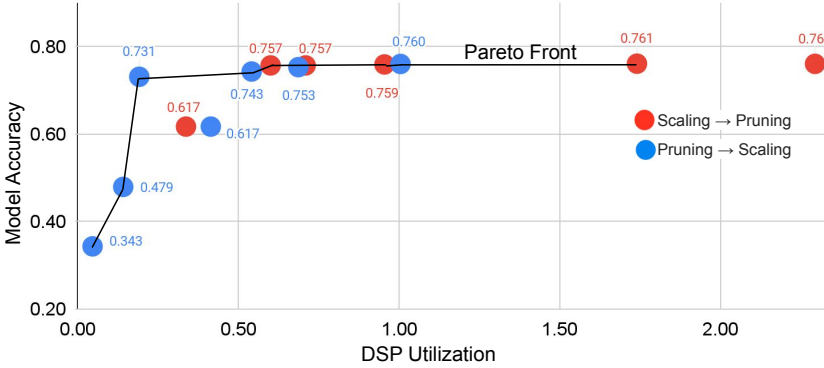


Fig. 13. Pareto Front meta-model designs post REDUCE  $K$ -task, color-coded paths.

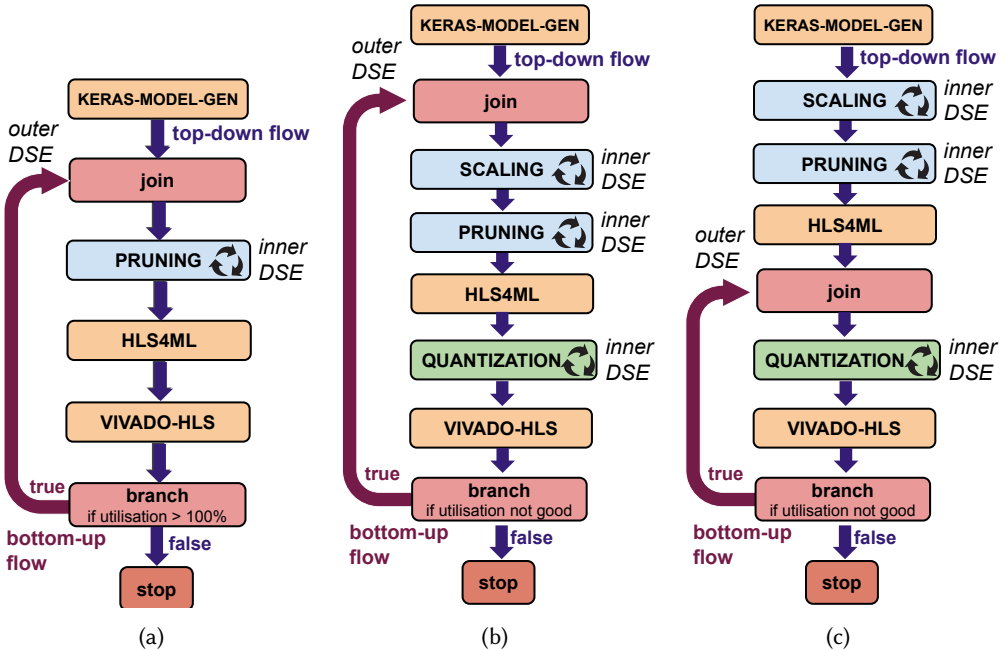
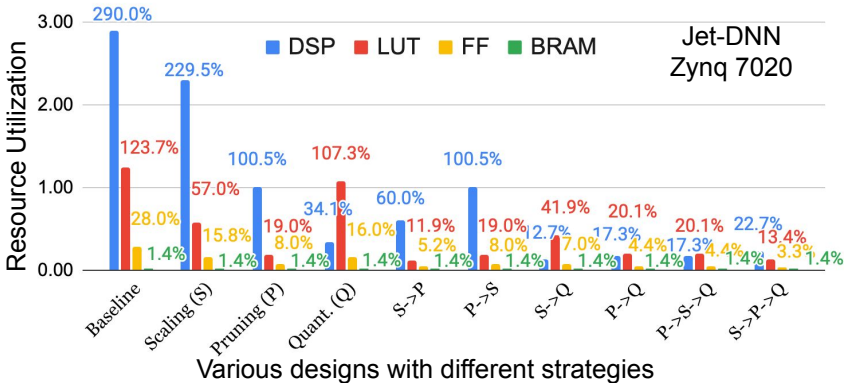


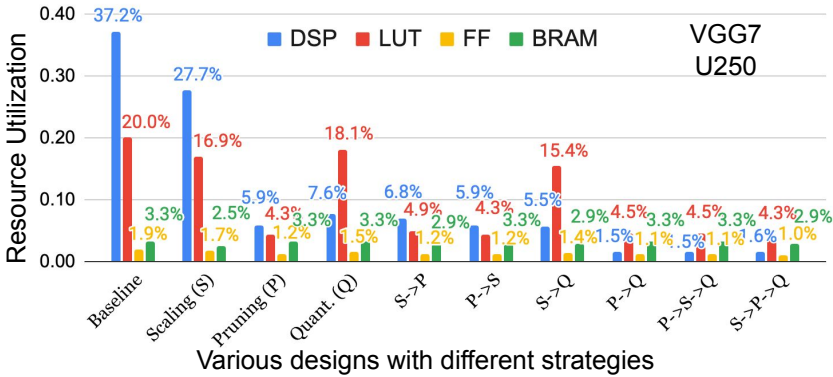
Fig. 14. (a) Pruning strategy with Branch. (b) Combined strategy with Branch to python (SW) space. (c) The combined strategy with Branch to HLS space.

### 5.6 Bottom-up Flows

Fig 14 reveal two distinct flows in the optimization strategies: top-down, where information flows from the DNN to the hardware stage, and bottom-up, the reverse. We have automated both flows by customizing the  $K$ -task BRANCH with a user-defined predicate function to activate or stop the bottom-up flow if the resulting design overmaps. The BRANCH task also support a user-supplied action function that is triggered when the predicate condition is true. For our current strategies, the action function changes the CFG section of the meta-model, increasing the accuracy tolerance parameters  $\alpha_p$ ,  $\alpha_s$ , and  $\alpha_q$  (if applicable) for the next iteration. Note that our current strategies in Fig. 14 have two DSE loops: an inner-loop that is codified within each  $O$ -task and an outer-loop supported by the bottom-up flow. Users can develop more complex strategies by customizing the outer loop, for instance, by updating the bottom-up condition and parameter tuning.



(a)



(b)

Fig. 15. (a) The hardware resources and latency of the Jet-DNN designs after various strategies. (b) The hardware resources and latency of the VGG7 designs after various strategies.

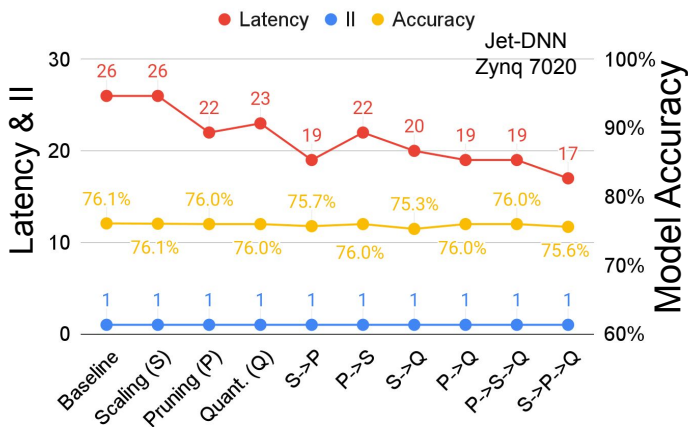


Fig. 16. Latency, Initiation Interval (II) and model accuracy of various designs with different strategies

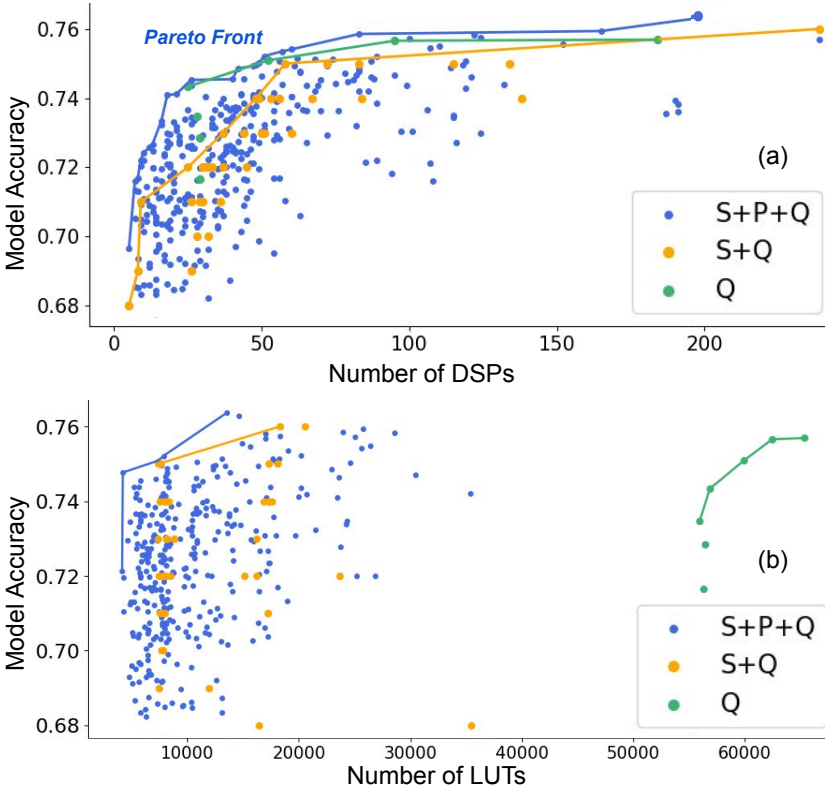


Fig. 17. Comparison of Pareto frontiers of **JetDNN** model accuracy and resource utilization using different optimization strategies.

### 5.7 Optimization strategy search - combination and order

Combining optimization methods increases diversity and potential designs, improving optimal balance between accuracy and efficiency. We systematically evaluate all candidates combined optimization strategies based on our current set of 3 optimization tasks, Scaling (**S**), Pruning (**P**), and Quantization (**Q**), to identify the most effective combination and order. The  $\alpha_p$ ,  $\alpha_s$  and  $\alpha_q$  are set to 2%, 0.05% and 1%. In particular, Fig 15(a) shows the hardware resource utilization results after each strategy and Fig 16 shows the corresponding latency, initiation interval and model accuracy. The final optimized model of Jet-DNN after scaling, pruning and quantization is depicted as “S→P→Q” design, resulting in a reduction of the DSP usage by around 92% and LUT usage by around 89% compared with the original design (baseline [7, 27]). In addition, the latency is reduced by 35% while the accuracy loss is trivial, as shown in Fig 16. The same search is performed on the VGG7 network with results shown in Fig. 15(b). The final design reduces DSP usage by a factor of 23 with the same latency and around 1.1% accuracy loss compared with the baseline design.

The search for optimal combinations and sequences with multiple *O*-tasks can be computationally demanding due to the exponential growth of the search space with the number of *O*-tasks. Advanced search methods can replace the current brute-force search. Recent studies [8, 18, 44] demonstrate surrogate models can expedite the search. Our framework facilitates the deployment of such techniques, enabling users to interface a search algorithm with the hardware design with minimal programming effort.

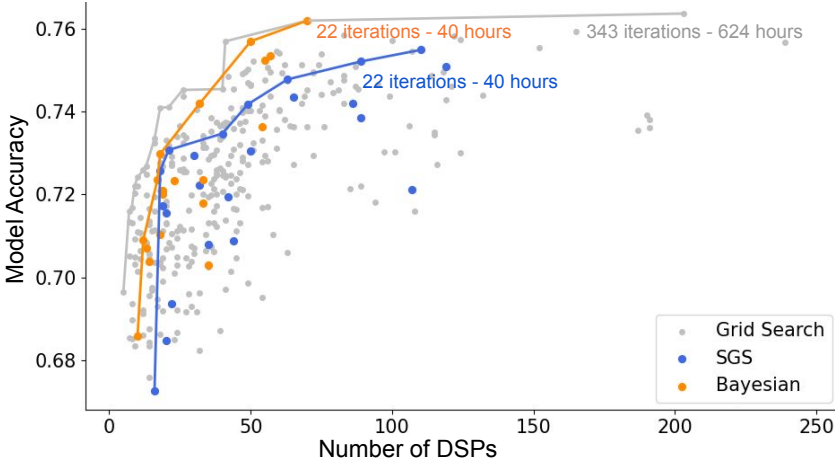


Fig. 18. DSP-Accuracy Pareto frontiers for each optimization using different DSE methods for **JetDNN** models.

### 5.8 Optimization strategy search - tolerable loss variation

This subsection evaluate the performance and efficiency trade-offs when using different values for the maximum tolerable accuracy loss ( $\alpha_p$ ,  $\alpha_s$  and  $\alpha_q$ ) for each optimization task to determine the effectiveness of their combination. We compare three strategies: **Q**, **S**→**Q**, and **S**→**P**→**Q**, using Grid Search to create a Pareto frontier by assessing model accuracy against DSP and LUT utilization. As illustrated in Fig. 17, our findings reveal that the **S**→**P**→**Q** strategy outperforms both the **S**→**Q** and **Q** strategies across multiple dimensions, including accuracy, DSP and LUT usage. However, it is important to note that the **S**→**P**→**Q** strategy is less efficient in terms of time and design space requirements, demanding 220.5 times more time than the **Q** strategy. Practical applications may require a balance between performance, hardware resource utilization, and time investment, with the choice of strategy complexity and design space contingent on the specific use case. Our following experiments in this paper build on these findings, focusing on the **S**→**P**→**Q** strategy.

### 5.9 DSE Strategies

Finding the optimal designs with grid search is time-consuming, as discussed in the previous section. This section investigates various DSE algorithms, including grid search, stochastic grid search (SGS), and Bayesian optimization. Fig. 18 presents the results. Each colored dot represents an design at a specific iteration, with different colors indicating different algorithms. The solid lines represent the Pareto Frontier of each algorithm over iterations, with each colored line corresponding to 22 iterations taking 40 hours. The uppermost grey line indicates a total of 343 iterations using extensive grid search over 624 hours, representing a baseline for comparison. The Bayesian optimization achieves similar results with just 22 iterations, significantly reducing processing time by a factor of 15.6 compared to Grid Search. Compared to SGS, Bayesian optimization's efficient parameter search yields multiple points near the Pareto frontier, indicating its effectiveness in finding optimal designs and approaching global optima. This effective parameter search by employing past results demonstrates the robustness of the Bayesian optimization approach, enabling users to optimize models while minimizing time and effort.

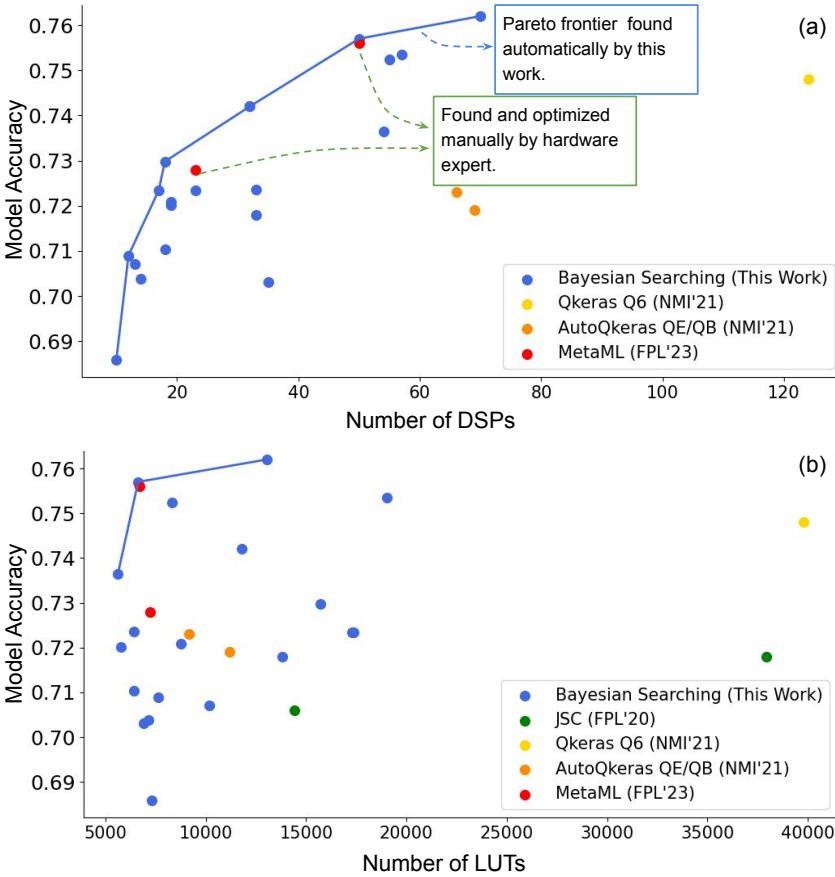


Fig. 19. Comparison of resource utilization of the FPGA-based **JetDNN** networks using our approach and others (LogicNets JSC [38], Qkeras Q6 [5], AutoQkeras QE/QB [5] and MetaML [27]) on an AMD/Xilinx VU9P FPGA. The Pareto frontier is highlighted.

### 5.10 Discussion and Comparison

Our evaluation results indicate that our combined *O*-task optimization strategy typically outperforms single *O*-task techniques. Furthermore, the order in which these optimization techniques are applied plays a crucial role, as different orders produce varying final results, as depicted in Fig. 15.

To highlight the advantages of our framework, we compare our results to those from other approaches targeting low-latency, low-resource, fully unfolded FPGA implementation of the JetDNN network, including LogicNets [38] JSC-M and JSC-L, QKeras-based Q6 [5], AutoQKeras-based QE and QB [5], and MetaML [27] in Fig. 19 and Table 4. All designs use the same architecture, except for JSC-L, which employs a larger architecture.

Compared to original Jet-DNN [7], our design achieves higher accuracy (up to 76.2%) while using less hardware resources. When compared with LogicNets JSC-M and JSC-L [38], which achieve accuracies of 70.6% and 71.8% respectively, our design demonstrates up to 5.6% higher accuracy while also offering resource efficiency. Against the AutoQkeras Q6 and QE designs [5], which yield accuracies of 74.8% and 72.3% respectively, our framework attains higher accuracy and lower latency while providing more granular trade-offs between resource utilization and latency. Compared to MetaML [27] with manual optimization, our work achieves comparable or better accuracy across various configurations with automatic optimization. Overall, the versatility of

Table 4. Performance comparison with the FPGA designs of Jet-DNN network using other approaches on Xilinx FPGAs with a clock frequency of 200MHz.

Model	$\alpha_s, \alpha_p, \alpha_q$ (%, %, %)	FPGA	Acc. (%)	Lat. (ns)	DSP (%)	LUT (%)
HLS4ML Jet-DNN [7]	-	KU115	75	75	954 (17.3)	-
FPL'20 [38] LogicNets JSC-M	-	VU9P	70.6	NA	0 (0)	14,428 (1.2)
FPL'20 [38] LogicNets JSC-L	-	VU9P	71.8	13 <sup>a</sup>	0 (0)	37,931 (3.2)
NMI'21 [5] Qkeras Q6	-	VU9P	74.8	55	124 (1.8)	39,782 (3.4)
NMI'21 [5] AutoQkeras QE	-	VU9P	72.3	55	66 (1.0)	9,149 (0.8)
NMI'21 [5] AutoQkeras QB	-	VU9P	71.9	70	69 (1.0)	11,193 (0.9)
FPL'23 [27] MetaML	-	VU9P	76.1	70	638 (9.3)	69,751 (5.9)
FPL'23 [27] MetaML	{0.05, 2, 1}	VU9P	75.6	45	50 (0.7)	6,698 (0.6)
FPL'23 [27] MetaML	{0.05, 2, 4}	VU9P	72.8	40	23 (0.2)	7,224 (0.6)
This work <b>(Best Acc.)</b>	{0.5, 0.1, 0.1}	VU9P	<b>76.2</b>	55	272 (4.0)	14,580 (1.2)
This work <b>(Best DSP)</b>	{0.5, 3, 4}	VU9P	69.7	40	<b>5</b> (0.1)	9,026 (0.8)
This work <b>(Best LUT)</b>	{2, 5, 1}	VU9P	72.1	45	47 (0.7)	<b>4,410</b> (0.4)
This work <sup>b</sup> <b>(Acc.-DSP-LUT)</b>	{0.5, 2, 0.5}	VU9P	<b>76.1</b>	50	<b>70</b> (1.0)	<b>13,042</b> (1.1)
This work <sup>b</sup> <b>(Acc.-DSP-LUT)</b>	{4, 0.5, 0.5}	VU9P	<b>75.7</b>	45	<b>50</b> (0.7)	<b>6,634</b> (0.6)
This work <sup>c</sup> <b>(Acc.-LUT)</b>	{4, 4, 0.5}	VU9P	<b>73.7</b>	45	54 (0.8)	<b>5,624</b> (0.5)
This work <sup>d</sup> <b>(Acc.-DSP)</b>	{2, 3, 4}	VU9P	<b>70.9</b>	40	<b>12</b> (0.2)	7,637 (0.8)

<sup>a</sup> A clock frequency of 384 MHz is used and the final softmax layer is removed.

<sup>b</sup> On both Accuracy-DSP and Accuracy-LUT Pareto lines as shown in Fig 19.

<sup>c</sup> Only on Accuracy-LUT Pareto line. <sup>d</sup> Only on Accuracy-DSP Pareto line.

our design, which balances accuracy, latency, and resource utilization across different objectives, highlights its superiority and adaptability for diverse FPGA-based DNN applications.



This effective parameter search demonstrates the robustness of the Bayesian Optimization approach, enabling users to optimize models while minimizing development time. Besides, this work demonstrates flexibility and effectiveness by achieving competitive performance across multiple configurations, highlighting its adaptability to different optimization priorities such as Accuracy, DSP and LUT. It is worth noting that our results are identified automatically while the other approaches involve manual optimization by DNN and hardware experts.

## 6 CONCLUSION

This paper presents a novel co-optimization framework for FPGA-based DNN accelerators, which comprises building blocks that facilitate rapid development of customized cross-stage design flows, automating the entire design iteration process. The results demonstrate that our approach significantly reduces DSP resource usage by up to 92% and LUT usage by up to 89%, while maintaining accuracy, without requiring human effort or domain expertise. In addition, our results reveal that Bayesian optimization in DSE significantly streamlines the process, achieving results comparable to grid search but with a 15.6-fold reduction in processing time. Our futurework will extend this approach to include RTL space, support more DNN architectures, including Variational Autoencoder (VAE) [25] and transformer [43] networks, and incorporate more optimization strategies like balancing initiation interval [29, 32] for further improvements in hardware efficiency and model performance.

**Acknowledgement:** The support of the United Kingdom EPSRC (grant numbers EP/V028251/1, EP/L016796/1, EP/N031768/1, EP/P010040/1, EP/S030069/1, and EP/X036006/1), Intel, and AMD is gratefully acknowledged. We thank Markus Roglien, Shuo Liu and Anyan Zhao for their help.

## REFERENCES

- [1] 2023. OpenVINO toolkit. <https://github.com/openvinotoolkit/openvino>.
- [2] Mohamed S Abdelfattah, Lukasz Dudziak, Thomas Chau, Royson Lee, Hyeji Kim, and Nicholas D Lane. 2020. Best of both worlds: Automl codesign of a cnn and its hardware accelerator. In *2020 57th ACM/IEEE Design Automation Conference (DAC)*. IEEE, 1–6.
- [3] Nicolas Bohm Agostini, Serena Curzel, Vinay Amatya, Cheng Tan, Marco Minutoli, Vito Giovanni Castellana, Joseph Manzano, David Kaeli, and Antonino Tumeo. 2022. An MLIR-based Compiler Flow for System-Level Design and Hardware Acceleration. In *Proceedings of the 41st IEEE/ACM International Conference on Computer-Aided Design*. 1–9.
- [4] Tianqi Chen, Thierry Moreau, Ziheng Jiang, Lianmin Zheng, Eddie Yan, Haichen Shen, Meghan Cowan, Leyuan Wang, Yuwei Hu, Luis Ceze, et al. 2018. {TVM}: An automated {End-to-End} optimizing compiler for deep learning. In *13th USENIX Symposium on Operating Systems Design and Implementation (OSDI 18)*. 578–594.
- [5] Claudionor N Coelho, Aki Kuusela, Shan Li, Hao Zhuang, Jennifer Ngadiuba, Thea Klæboe Aarrestad, Vladimir Loncar, Maurizio Pierini, Adrian Alan Pol, and Sioni Summers. 2021. Automatic heterogeneous quantization of deep neural networks for low-latency inference on the edge for particle detectors. *Nature Machine Intelligence* 3, 8 (2021), 675–686.
- [6] Zhen Dong, Yizhao Gao, Qijing Huang, John Wawrzynek, Hayden KH So, and Kurt Keutzer. 2021. Hao: Hardware-aware neural architecture optimization for efficient inference. In *2021 IEEE 29th Annual International Symposium on Field-Programmable Custom Computing Machines (FCCM)*. IEEE, 50–59.
- [7] Javier Duarte, Song Han, Philip Harris, Sergo Jindariani, Edward Kreinar, Benjamin Kreis, Jennifer Ngadiuba, Maurizio Pierini, Ryan Rivera, Nhan Tran, et al. 2018. Fast inference of deep neural networks in FPGAs for particle physics. *Journal of Instrumentation* 13, 07 (2018), P07027.
- [8] Lorenzo Ferretti, Andrea Cini, Georgios Zacharopoulos, Cesare Alippi, and Laura Pozzi. 2022. Graph Neural Networks for High-Level Synthesis Design Space Exploration. *ACM Transactions on Design Automation of Electronic Systems* 28, 2 (2022), 1–20.
- [9] Fumio Hamanaka, Takashi Odan, Kenji Kise, and Thiem Van Chu. 2023. An Exploration of State-of-the-art Automation Frameworks for FPGA-based DNN Acceleration. *IEEE Access* (2023).
- [10] Cong Hao and Deming Chen. 2018. Deep neural network model and FPGA accelerator co-design: Opportunities and challenges. In *2018 14th IEEE International Conference on Solid-State and Integrated Circuit Technology (ICSICT)*. IEEE, 1–4.

- [11] Cong Hao, Yao Chen, Xinheng Liu, Atif Sarwari, Daryl Sew, Ashutosh Dhar, Bryan Wu, Dongdong Fu, Jinjun Xiong, Wen-mei Hwu, et al. 2019. NAIS: Neural architecture and implementation search and its applications in autonomous driving. In *2019 IEEE/ACM International Conference on Computer-Aided Design (ICCAD)*. IEEE, 1–8.
- [12] Cong Hao, Yao Chen, Xiaofan Zhang, Yuhong Li, Jinjun Xiong, Wen-mei Hwu, and Deming Chen. 2020. Effective algorithm-accelerator co-design for ai solutions on edge devices. In *Proceedings of the 2020 on Great Lakes Symposium on VLSI*. 283–290.
- [13] Cong Hao, Jordan Dotzel, Jinjun Xiong, Luca Benini, Zhiru Zhang, and Deming Chen. 2021. Enabling design methodologies and future trends for edge AI: specialization and codesign. *IEEE Design & Test* 38, 4 (2021), 7–26.
- [14] Cong Hao, Xiaofan Zhang, Yuhong Li, Sitao Huang, Jinjun Xiong, Kyle Rupnow, Wen-mei Hwu, and Deming Chen. 2019. FPGA/DNN co-design: An efficient design methodology for 1ot intelligence on the edge. In *2019 56th ACM/IEEE Design Automation Conference (DAC)*. IEEE, 1–6.
- [15] Kaiming He, Xiangyu Zhang, Shaoqing Ren, and Jian Sun. 2016. Deep residual learning for image recognition. In *Proceedings of the IEEE conference on computer vision and pattern recognition*. 770–778.
- [16] Weiwen Jiang, Lei Yang, Edwin Hsing-Mean Sha, Qingfeng Zhuge, Shouzhen Gu, Sakyaingha Dasgupta, Yiyu Shi, and Jingtong Hu. 2020. Hardware/software co-exploration of neural architectures. *IEEE Transactions on Computer-Aided Design of Integrated Circuits and Systems* 39, 12 (2020), 4805–4815.
- [17] Vinod Kathail. 2020. Xilinx vitis unified software platform. In *Proceedings of the 2020 ACM/SIGDA International Symposium on Field-Programmable Gate Arrays*. 173–174.
- [18] Maciej Kurek, Marc Peter Deisenroth, Wayne Luk, and Timothy Todman. 2016. Knowledge transfer in automatic optimisation of reconfigurable designs. In *2016 IEEE 24th Annual International Symposium on Field-Programmable Custom Computing Machines (FCCM)*. IEEE, 84–87.
- [19] Yann LeCun, Yoshua Bengio, and Geoffrey Hinton. 2015. Deep learning. *nature* 521, 7553 (2015), 436–444.
- [20] Yann LeCun, Léon Bottou, Yoshua Bengio, and Patrick Haffner. 1998. Gradient-based learning applied to document recognition. *Proc. IEEE* 86, 11 (1998), 2278–2324.
- [21] Atefeh Mehrabi, Aninda Manocha, Benjamin C Lee, and Daniel J Sorin. 2020. Bayesian optimization for efficient accelerator synthesis. *ACM Transactions on Architecture and Code Optimization (TACO)* 18, 1 (2020), 1–25.
- [22] Eric A Moreno, Olmo Cerri, Javier M Duarte, Harvey B Newman, Thong Q Nguyen, Avikar Periwal, Maurizio Pierini, Aidana Serikova, Maria Spiropulu, and Jean-Roch Vlimant. 2020. JEDI-net: a jet identification algorithm based on interaction networks. *The European Physical Journal C* 80, 1 (2020), 1–15.
- [23] Yuval Netzer, Tao Wang, Adam Coates, Alessandro Bissacco, Bo Wu, and Andrew Y Ng. 2011. Reading digits in natural images with unsupervised feature learning. (2011).
- [24] Jonas Ney, Dominik Loroeh, Vladimir Rybalkin, Nico Weber, Jens Krüger, and Norbert Wehn. 2021. HALF: Holistic auto machine learning for FPGAs. In *2021 31st International Conference on Field-Programmable Logic and Applications (FPL)*. IEEE, 363–368.
- [25] Zhiqiang Que et al. 2024. Low Latency Variational Autoencoder on FPGAs. *IEEE Journal on Emerging and Selected Topics in Circuits and Systems* (2024).
- [26] Zhiqiang Que, Jose GF Coutinho, and Wayne Luk. 2024. Deep Learning Design-Flow with Static and Dynamic Optimizations. In *2024 IEEE 17th International Conference on Solid-State & Integrated Circuit Technology (ICSICT)*. IEEE, 1–4.
- [27] Zhiqiang Que, Shuo Liu, Markus Rognlien, Ce Guo, Jose GF Coutinho, and Wayne Luk. 2023. MetaML: Automating Customizable Cross-Stage Design-Flow for Deep Learning Acceleration. In *2023 30th International Conference on Field-Programmable Logic and Applications (FPL)*. IEEE.
- [28] Zhiqiang Que, Hiroki Nakahara, Eriko Nurvitadhi, Hongxiang Fan, Chenglong Zeng, Jiuxi Meng, Xinyu Niu, and Wayne Luk. 2020. Optimizing Reconfigurable Recurrent Neural Networks. In *IEEE 28th Annual International Symposium on Field-Programmable Custom Computing Machines (FCCM)*. IEEE, 10–18.
- [29] Zhiqiang Que, Erwei Wang, Umar Marikar, Eric Moreno, Jennifer Ngadiuba, Hamza Javed, Bartłomiej Borzyszkowski, Thea Arrestad, Vladimir Loncar, Sioni Summers, et al. 2021. Accelerating recurrent neural networks for gravitational wave experiments. In *2021 IEEE 32nd International Conference on Application-specific Systems, Architectures and Processors (ASAP)*. IEEE, 117–124.
- [30] Zhiqiang Que, Anyan Zhao, Jose GF Coutinho, Ce Guo, and Wayne Luk. 2024. Optimizing DNN Accelerator Compression Using Tolerable Accuracy Loss. In *International conference on field-programmable technology (FPT)*. IEEE.
- [31] Brandon Reagen, José Miguel Hernández-Lobato, Robert Adolf, Michael Gelbart, Paul Whatmough, Gu-Yeon Wei, and David Brooks. 2017. A case for efficient accelerator design space exploration via bayesian optimization. In *2017 IEEE/ACM International Symposium on Low Power Electronics and Design (ISLPED)*. IEEE, 1–6.
- [32] Markus Rognlien, Zhiqiang Que, Jose GF Coutinho, and Wayne Luk. 2022. Hardware-aware optimizations for deep learning inference on edge devices. In *International Symposium on Applied Reconfigurable Computing*. Springer, 118–133.

- [33] Karen Simonyan and Andrew Zisserman. 2014. Very deep convolutional networks for large-scale image recognition. *arXiv preprint arXiv:1409.1556* (2014).
- [34] Atefeh Sohrabzadeh, Yunsheng Bai, Yizhou Sun, and Jason Cong. 2022. Automated accelerator optimization aided by graph neural networks. In *Proceedings of the 59th ACM/IEEE Design Automation Conference*. 55–60.
- [35] Vivienne Sze, Yu-Hsin Chen, Tien-Ju Yang, and Joel S Emer. 2017. Efficient processing of deep neural networks: A tutorial and survey. *Proc. IEEE* 105, 12 (2017), 2295–2329.
- [36] Stephen Tridgell, Martin Kumm, Martin Hardieck, David Boland, Duncan Moss, Peter Zipf, and Philip HW Leong. 2019. Unrolling Ternary Neural Networks. *ACM Transactions on Reconfigurable Technology and Systems (TRETS)* 12, 4 (2019), 1–23.
- [37] Shikhar Tuli, Chia-Hao Li, Ritvik Sharma, and Niraj K Jha. 2023. CODEBench: A neural architecture and hardware accelerator co-design framework. *ACM Transactions on Embedded Computing Systems* 22, 3 (2023), 1–30.
- [38] Yaman Umuroglu, Yash Akhauri, Nicholas James Fraser, and Michaela Blott. 2020. LogicNets: co-designed neural networks and circuits for extreme-throughput applications. In *2020 30th International Conference on Field-Programmable Logic and Applications (FPL)*. IEEE, 291–297.
- [39] Yaman Umuroglu, Nicholas J Fraser, Giulio Gambardella, Michaela Blott, Philip Leong, Magnus Jahre, and Kees Vissers. 2017. FINN: A framework for fast, scalable binarized neural network inference. In *Proceedings of the 2017 ACM/SIGDA international symposium on field-programmable gate arrays*. 65–74.
- [40] Jessica Vandebon, Jose G. F. Coutinho, Wayne Luk, Eriko Nurvitadhi, and Tim Todman. 2020. Artisan: a Meta-Programming Approach For Codifying Optimisation Strategies. In *2020 IEEE 28th Annual International Symposium on Field-Programmable Custom Computing Machines (FCCM)*.
- [41] Stylianos I Venieris and Christos-Savvas Bouganis. 2016. fpgaConvNet: A framework for mapping convolutional neural networks on FPGAs. In *2016 IEEE 24th Annual International Symposium on Field-Programmable Custom Computing Machines (FCCM)*. IEEE, 40–47.
- [42] Erwei Wang, James J Davis, Ruizhe Zhao, Ho-Cheung Ng, Xinyu Niu, Wayne Luk, Peter YK Cheung, and George A Constantinides. 2019. Deep neural network approximation for custom hardware: Where we’ve been, where we’re going. *ACM Computing Surveys (CSUR)* 52, 2 (2019), 1–39.
- [43] Filip Wojcicki, Zhiqiang Que, Alexander D Tapper, and Wayne Luk. 2022. Accelerating transformer neural networks on fpgas for high energy physics experiments. In *2022 International Conference on Field-Programmable Technology (ICFPT)*. IEEE, 1–8.
- [44] Nan Wu, Yuan Xie, and Cong Hao. 2021. Ironman: GNN-assisted design space exploration in high-level synthesis via reinforcement learning. In *Proceedings of the 2021 on Great Lakes Symposium on VLSI*. 39–44.
- [45] Pengfei Xu, Xiaofan Zhang, Cong Hao, Yang Zhao, Yongan Zhang, Yue Wang, Chaojian Li, Zetong Guan, Deming Chen, and Yingyan Lin. 2020. AutoDNNchip: An automated DNN chip predictor and builder for both FPGAs and ASICs. In *Proceedings of the 2020 ACM/SIGDA International Symposium on Field-Programmable Gate Arrays*. 40–50.
- [46] Yifan Yang, Qijing Huang, Bichen Wu, Tianjun Zhang, Liang Ma, Giulio Gambardella, Michaela Blott, Luciano Lavagno, Kees Vissers, John Wawrzyniek, et al. 2019. Synetgy: Algorithm-hardware co-design for convnet accelerators on embedded fpgas. In *Proceedings of the 2019 ACM/SIGDA international symposium on field-programmable gate arrays*. 23–32.
- [47] Hanchen Ye, Cong Hao, Jianyi Cheng, Hyunmin Jeong, Jack Huang, Stephen Neuendorffer, and Deming Chen. 2022. Scalehls: A new scalable high-level synthesis framework on multi-level intermediate representation. In *2022 IEEE International Symposium on High-Performance Computer Architecture (HPCA)*. IEEE, 741–755.
- [48] Chen Zhang, Peng Li, Guangyu Sun, Yijin Guan, Bingjun Xiao, and Jason Cong. 2015. Optimizing FPGA-based accelerator design for deep convolutional neural networks. In *Proceedings of the 2015 ACM/SIGDA international symposium on field-programmable gate arrays*. 161–170.
- [49] Xiaofan Zhang, Yuhong Li, Junhao Pan, and Deming Chen. 2022. Algorithm/Accelerator Co-Design and Co-Search for Edge AI. *IEEE Transactions on Circuits and Systems II: Express Briefs* 69, 7 (2022), 3064–3070.
- [50] Xiaofan Zhang, Hanchen Ye, Junsong Wang, Yonghua Lin, Jinjun Xiong, Wen-mei Hwu, and Deming Chen. 2020. DNNExplorer: a framework for modeling and exploring a novel paradigm of FPGA-based DNN accelerator. In *Proceedings of the 39th International Conference on Computer-Aided Design*. 1–9.